

Determination of flow configurations and fluid forces acting on two tandem square cylinders in cross-flow and its wake patterns

A. Etminan*, M. Moosavi and N. Ghaedsharafi

Mechanical Engineering Department, Islamic Azad University, Neyriz Branch, Neyriz, Iran

*corresponding author's e-mail: iautech.etminan@iauneyriz.ac.ir

Abstract— In this paper, the onset of vortex shedding and flow configurations over two equal square cylinders in tandem arrangement are carried out on a finite volume code based on the SIMPLEC algorithm and non-staggered mesh for both steady and unsteady incompressible laminar flow in the two dimensional regime. The calculations are performed for a Reynolds number range varying from 1 to 200 and spacing between the cylinders is five widths of the cylinders. The mesh is finer close to the cylinders walls in order to have a better description of boundary layer. In this research, the influence of Reynolds number and the onset of vortex shedding on the flow patterns around the cylinders are presented in detail. In addition, the quantities such as pressure and viscous drag coefficients, RMS lift and drag coefficients, recirculation length and phase lag are presented and explained. It is found that the onset of vortex shedding occurs for a Reynolds number varying 35 to 40.

Keywords—Control Volume, Laminar Flow, Square Cylinder, Unsteady Flow, Vortex Shedding.

I. INTRODUCTION

THE main anxiety about flexible structures exposed to the flow is vibration and fluctuating forces which are caused by vortex shedding phenomenon. The interaction of the flow about groups of cylinders is becoming an increasingly popular field of many studies. Flow interference is responsible for several changes in the characteristics of the flow around pairs of cylinders which can provide a better understanding of the vortex shedding and aerodynamic forces, in cases involving more complex arrangements. Some examples including; group of electrical transmission lines, tall buildings and skyscrapers in a city, cooling towers, chimneys, pipelines, cables and bundles of tubes in heat exchangers. These flows usually include some complex events such as separation flow, wake region, shear flow and eddy shedding.

Square cylindrical geometries often appear in many structures and industrial applications. Although these structures are very simple, the flow pattern around them is not. The square cylinder is a bluff body and can forms a large separated region and a massive unsteady wake downstream. Separated wake and its patterns are nearly impossible to predict analytically and hence must be solved either through experimental and numerical methods.

It seems that is some similarity between the flow structures of the single and tandem cylinders. Zdravkovich [1], [2] has reviewed the problem of flow interference when two cylinders are placed in side-by-side, tandem and staggered arrangements in a steady flow. Quoting his words, he observed that “when more than one bluff body is placed in a fluid flow, the resulting forces and vortex shedding patterns may be completely different from those found on a single body at the same Reynolds number”. A variety of flow patterns, characterized by the behaviour of the wake region, may be discerned as the spacing between two square cylinders is changed. The large separated wakes from each of the square cylinders interact with each other to form a flow that is greatly different than the flow around a single cylinder. The exact form of the interaction is highly dependent on the Reynolds number of the flow and on the cylinder placement.

Mani and Mahjoob [3] compared aerodynamic performances of two set finned bodies with circular and non-circular cross sections. They studied flows over two circular and square bodies with rounded corners, which are attached to two fins in the free stream Mach number of 0.83 experimentally and numerically. The experiment data in different angles of attack indicate that the square fin body configuration has higher aerodynamic lift and drag coefficients than the circular one. Also, the results indicate the same aerodynamic performance for both bodies. The results of CFD confirm the deduction obtained from experiment and, also they explain the aerodynamic parameters of different parts of fin-body configurations which are very important.

Portugaels *et al.* [4] determined aerodynamic force coefficient acting on octagonal lighting columns experimentally. The aerodynamic forces induced by the wind on octagonal cylindrical elements with different diameters, different edge curvature radii and different roughness have been measured in a wind tunnel in order to determine the influence of these parameters on the aerodynamic force coefficients. Their database showed that the force coefficients for octagonal cylinders depend strongly on the surface roughness and rounded edge radius. They are also more important than for the circular cylinders, especially at high Reynolds number.

S.R Sabbagh *et al.* [5] numerically simulated the wind around circular cylinder. They solved two dimensional Navier-Stokes equations for an incompressible fluid combined with a SGS eddy viscosity model to simulate turbulent. Their computed results are presented in terms of color coded maps of pressure and velocity fields as well as velocity vectors on boundary surfaces of the solution domain. The results show that, there are differences in computed pressure fields on the wall surface of the circular cylinder due to application of SGS turbulent eddy viscosity model.

Benra and Dohmen [6] numerically simulated interaction between fluid and structures with square cross section. They found the fundamental relations for the calculation of the flow behavior and of the structure dynamics.

The literature review has been declared, there is a much shorter history of flow over two square cylinders than that of flow over a single square cylinder. The fundamental fluid dynamics problems of single circular and square cylinders have been examined extensively in both numerical and experimental studies [7]-[11]. Some of them reviewed results of numerical and experimental carried out over a wide range of Reynolds numbers and vortex shedding of more-or-less bluff bodies. Their results showed that the flow patterns around 2D bodies can be highly three-dimensional. Tatsutani, *et al.* [12] studied tandem square cylinders in a channel for Reynolds numbers between 200 and 1600 based on the downstream cylinder. They observed distinct flow patterns that are dependent on a critical inter-cylinder spacing. Below the critical spacing, two counter-rotating eddies formed in the gap between the square cylinders and vortex shedding was only observed for the downstream cylinder. At the critical spacing, vortex shedding was initiated for the upstream square cylinder. A reduction in the size of the eddy promoter caused an increase in the frequency of vortex shedding from the downstream square cylinder.

Flow structure and heat transfer from two equally sized tandem rectangular cylinders in a channel were numerically simulated by Valencia [13], [14]. He observed that the channel blockage ratio was the dominant parameter for heat transfer enhancement. He also found that, the drag coefficient and the pressure loss increases due to the existence of the rectangular cylinders in the channel.

Devarakonda and Humphrey [15] performed experimental and numerical investigations for the unsteady flow past a tandem pair of square cylinders for a Reynolds number of 592 based on the downstream cylinder. The presence of an eddy promoter enhanced the heat transfer of the downstream cylinder and reduced the drag experienced by the two cylinders. The channel flow had a uniform inlet profile.

Subsequently, Devarakonda [16] numerically showed that the heat transfer from the downstream cylinder was maximized for certain inter-cylinder separations. Configurations that yielded a negative or zero drag coefficient for the downstream square cylinders were also found.

A comprehensive review of earlier work on rectangular cylinders is available in Rosales *et al.* [17]. They numerically

simulated the fluid flow and the heat transfer around two square cylinders with different sizes and arrangements in a channel, $Re = 500$. In this study, the channel walls and the upstream cylinder are considered insulators whereas the downstream cylinder is hot. It was shown that the drag coefficient and the Nusselt number of downstream cylinder decrease, when the inline or offset tandem pair of cylinders is positioned closer to a channel wall.

Zhang *et al.* [18] and DeJong *et al.* [19] in their numerical and experimental model of offset-strip and louvered fins as a periodic inline and staggered array of rectangular cylinders, observed that the Karman vortices have a strong influence on heat transfer as they continually bring far-field fluid towards the cylinder surface and thereby thin the local thermal boundary layer. However, the associated pressure drop increases with the onset of vortex shedding. It is thus of interest to know when the onset of vortex shedding or Hopf bifurcation occurs in a periodic array of cylinders and how it is related to that of an isolated cylinder.

Liu and Chen [20] performed an experimental study on the flow over two unconfined square cylinders in a tandem arrangement, $Re = 2000 - 16000$. They reported that there is hysteresis with two discontinuous jumps, which is associated with two different flow patterns. The suppression of the fluid forces on the two square cylinders in a tandem arrangement in which a flow approaching the upstream cylinder was controlled by a flat plate was examined, with variation in spacing between the plate and upstream cylinder, $Re = 56000$ [21]. Two square cylinders were installed in tandem in a vertical water tank and the effects of Reynolds number, spacing ratio and rotation angle of the downstream cylinder on the flow characteristic modes, drag coefficients and the vortex shedding frequency were experimentally studied by Yen *et al.* [22]. Mizushima [23] are investigated the interactions of wakes in a flow past a row of square bars, which is placed across a uniform flow, by numerical simulations and experiments. They are found that the vortices are shed synchronously from adjacent square bars in the same phase or in anti-phase depending upon the distance between the bars. The critical Reynolds numbers of the transitions are evaluated numerically.

Although some information is available on the flow over two square cylinders in cross flow, virtually no analogous results are available for the very low-Reynolds number flow regime and its details such as separation point and the onset of unsteadiness. The objective of the present work is to study free-stream flow over two square cylinders and explore the link between fluctuating forces and the two dimensional laminar flow regimes for various Reynolds number. Although the flow regimes have been studied previously, the physics of flow patterns around two square cylinders, which is the focus of the present work, is largely unexplored. Another objective of this work is to generate a numerical database for the flow parameters with respect to the Reynolds number for the considered boundary conditions.

II. PROBLEM DESCRIPTION, NUMERICAL DETAILS, BOUNDARY CONDITIONS AND GOVERNING EQUATIONS

The problem under consideration is depicted in Figure 1. Two equal-sized tandem square cylinders with sides (d) are exposed at zero angle of attack to a constant free stream with uniform velocity represented by U_{in} . Incompressible viscous flow with the constant fluid properties is assumed. All dimensions are scaled with side (d). The vertical distance between the upper and lower boundaries, H , defines the blockage of the confined flow (blockage parameter, $B=d/H$). It is expected that if the width of the computational domain (H) is chosen adequately large, the lower blockage parameter, the flow in the lower and the upper boundaries goes to the free-stream conditions. In the other words, these boundaries should be sufficiently far away from the cylinders to satisfy this boundary condition. Reference [24] was studied the effect of blockage, for a single square cylinder. They have shown that the free-stream condition is satisfied and that the boundaries have little effect on the flow patterns if $B = 5\%$.

Also, Etminan [25] determined $B = 5\%$, i.e. $H = 20$ for two square cylinders to gaining the free stream conditions. In the present work, the blockage ratio is $B = 5\%$, The distance between the cylinders is selected as a constant value, i.e. $G = 5$, and the upstream and downstream distances of the computational domain are selected $X_u = 5$ and $X_d = 15$, respectively, see Figure 1. These values are chosen based on the accomplished studies in the mentioned references.

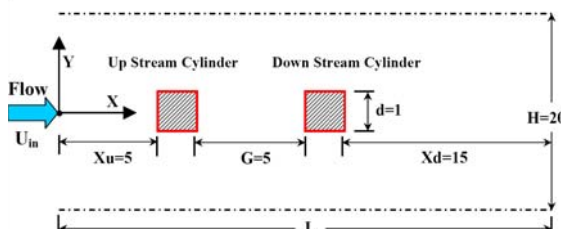


Fig. 1 Computational domain for flow around the square cylinders.

A typical generated grid is shown in Figure 2. Owing to the existence of the cylinders and their effect on the flow, a non-uniform grid is made around the cylinders using a hyperbolic tangent stretching function. This type of stretching functions and their advantages in non-uniform grid distribution have been discussed by Thompson *et al.* [26].

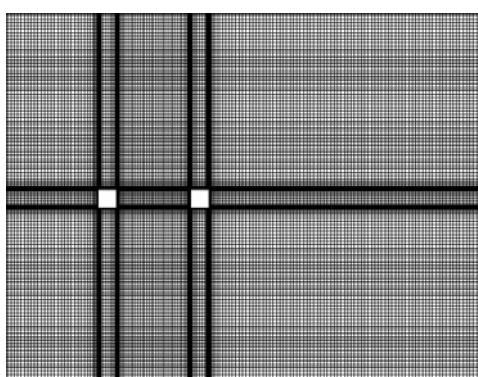


Fig. 2 Non-uniform computational grid structure.

Beyond this non-uniform region (one d from cylinders surfaces), a uniform grid is established with the same size as the latest generated cell in the places with non-uniform grid distribution. The distribution of control volume size in X and Y direction are shown in Figure 3. The domain is divided into five and three separate zones in X and Y directions respectively included both uniform and non-uniform grid zones. The grid distribution was made uniform with a constant cell size, 0.18, outside a region around the cylinder that extended upstream, downstream, and sideways. A grid of much smaller size, d , is clustered around the cylinder, with the smallest cell size, 0.0053, over a distance of one unit to adequately capture wake-wall interactions.

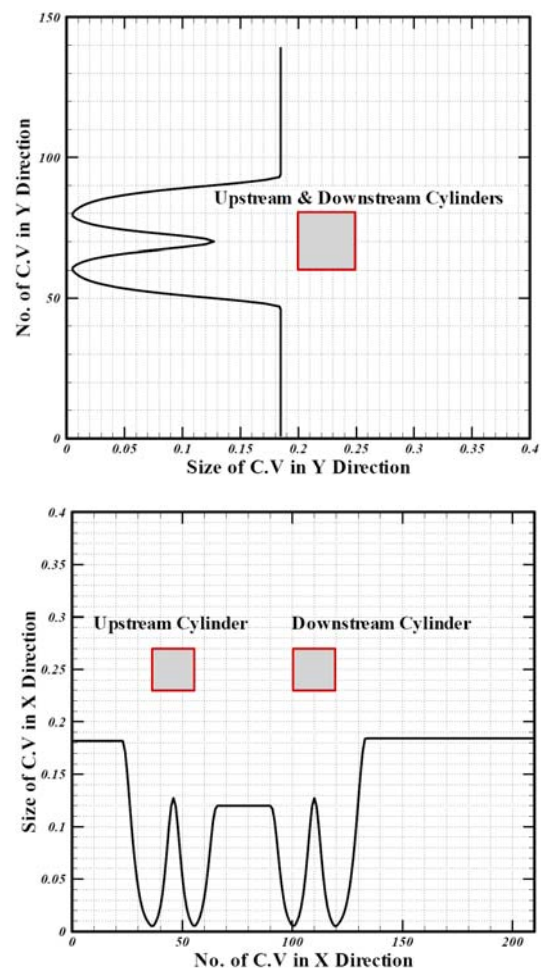


Fig. 3 The control volume size distributions: (a) in Y direction and (b) in X direction.

The employed boundary conditions are as follows:

Top and bottom boundaries: $\partial U / \partial Y = 0$, $V = 0$

No-slip condition on the cylinders walls: $U = V = 0$

Uniform velocity at the inlet: $U_{in} = 1$, $V_{in} = 0$

Outlet boundary condition: $\partial U / \partial X = 0$

The unsteady Navier-Stokes equations in dimensionless form for incompressible flow by constant properties assumption are given as follows:

$$\text{Continuity: } U_{i,i} = 0 \quad (1)$$

$$\text{Momentum: } U_{i,\tau} + (U_i U_j)_{,j} = -P_{,i} + \text{Re}^{-1} U_{i,jj} \quad (2)$$

Where,

$$\tau = \frac{t u_{in}}{d}, P = \frac{p}{\rho u_{in}^2}, U_i = \frac{u_i}{u_{in}} \quad i, j = 1, 2$$

All of the above equations are presented with regard to constant density and viscosity. The Reynolds number is defined as $\text{Re} = u_{in} d / \nu$. In above equations u_{in} , d , ρ and ν correspond to the inlet flow velocity, the side of cylinders, the frequency of vortex shedding, density and kinematic viscosity of fluid.

The total forces acting on cylinders that can be breakdown to the two components, e.g. drag and lift defines as follows:

$$\vec{F} = \vec{F}_{\text{Drag}} + \vec{F}_{\text{Lift}} \quad (3)$$

Also, the total drag and lift forces that can be divided to pressure and viscous components are given as follows:

$$F_{\text{Drag}(d)} = F_{\text{Pressure}(dp)} + F_{\text{Shear}(df)} \quad (4)$$

$$F_{\text{Lift}(l)} = F_{\text{Pressure}(lp)} + F_{\text{Shear}(lf)} \quad (5)$$

Now, the drag and lift coefficients are given as follows:

$$Cd = \frac{2F_d}{\rho u_{in}^2 d} = Cdp + Cdf \quad (6)$$

$$Cl = \frac{2F_l}{\rho u_{in}^2 d} = Clp + Clf \quad (7)$$

An incompressible SIMPLEC finite volume code is used employing collocated grid arrangement. The scheme is implicit in time, and a second order Crank-Nicolson scheme, has been used. The convective and diffusive terms are discretized using QUICK and central differencing schemes, respectively. The time-marching calculations are commenced with the fluid at rest and a constant time step $\Delta\tau = 0.025$ is used for all simulations. This value is chosen based on the presented numerical results by Sohankar [24] and the first author work [25].

III. RESULTS

In what follows, the both of steady and unsteady flow around two square cylinders in tandem arrangement are investigated for $\text{Re} = 1-200$ at $G = 5$. It is observed that the flow is steady for $\text{Re} \leq 35$ and it changes to unsteady for $\text{Re} \geq 40$. In the steady cases, the selected Reynolds numbers for the present study are 1, 2, and 5 to 35 in steps of 5 and the chosen Reynolds numbers in the unsteady cases are from 40 to 60 in steps of 5, from 60 to 100 in steps of 10 and from 100 to 200 in steps of 25. For all simulations, the distance between the cylinders is considered as $G = 5$. In the unsteady flow regime, the time-averaged quantities of the fluid flow parameters are calculated over approximately 20 shedding cycles in the saturated state where the starting processes are negligible. At the first next part, flow patterns are presented

and discussed, in that following, some global quantities versus the Reynolds number are studied.

Instantaneous streamlines colored by x-velocity component and vorticity contours around tandem cylinders are shown at nine instants during a period of the vortex shedding for $\text{Re} = 100$ in Figure 4. Owing to periodicity of the flow in the fully developed state, where the force signal amplitude reaches approximately to the constant levels, only nine instants during a shedding period are considered here. It is seen that a clockwise vortex is in development due to the separation at the upper rear corner of the upstream cylinder, see Figure 4(a,i). As it grows, with increasing strength but being fixed in position, the attachment point on the rear side is pushed downward, see Figures 4(b) and (c). As the attachment point more or less reaches to the lower rear corner at an instance between the corresponding time for Figures 4(c) and (d), a new anti-clockwise vortex is about to be formed at the lower rear corner, see Figure 4(e). As this new vortex grows, the old clockwise vortex is pushed away and is eventually shed into the wake of the upstream cylinder. In general, the same trend is also observed for the other time instants during the next half a shedding period but due to the separation occurs from the lower rear corner, see Figures 4(e-i).

Figure 5 shows instantaneous pressure contours around the cylinders when the maximum lift force acting on upstream and downstream cylinder for different Reynolds number. As mentioned that earlier, the lift force has two part namely, pressure and viscous components (see equations 5 and 7). The pressure lift has the main role in lift force acting on cylinders. Non uniform pressure distribution on cylinder's walls and vicinity of them, makes lift force. Also, from this figure can be found when maximum lift acts on upstream cylinder, the lift force acted on downstream is not at same phase. It is indicated phase lag, that will study at the following.

Figure 6 shows the steady and unsteady streamlines and vorticity contours around the cylinders for the different Reynolds numbers. At very low Reynolds numbers, the streamlines stick to both the cylinders walls completely and flow separation does not occur (see Figure 6 for $\text{Re} = 1$). As Reynolds number is increased, the flow is not fully attached and separation occurs. In this case, a pair of steady symmetric vortices forms behind the cylinders for $\text{Re} \geq 5$. At higher Reynolds numbers, the formation length of the recirculation region behind the cylinders grows and the vortices become stronger. At a critical Reynolds number approximately $\text{Re} = 35-40$, flow becomes unsteady and the vortex shedding occurs. This critical Reynolds number for the single square cylinder is reported in the range of $\text{Re} = 40-55$, [27]-[29].

For Reynolds number larger than the onset one, the twin vortex arrangement becomes unstable, and a time periodic oscillation wake and a staggered vortex street are formed from both the cylinders. For $\text{Re} \geq 40$ ($B=5\%$), the separated vortices are shed alternately from the upper and the lower side of the cylinders. For Reynolds number larger than the critical one, the time-averaged streamlines and vorticity contours are provided to gathered global quantities that presented later.

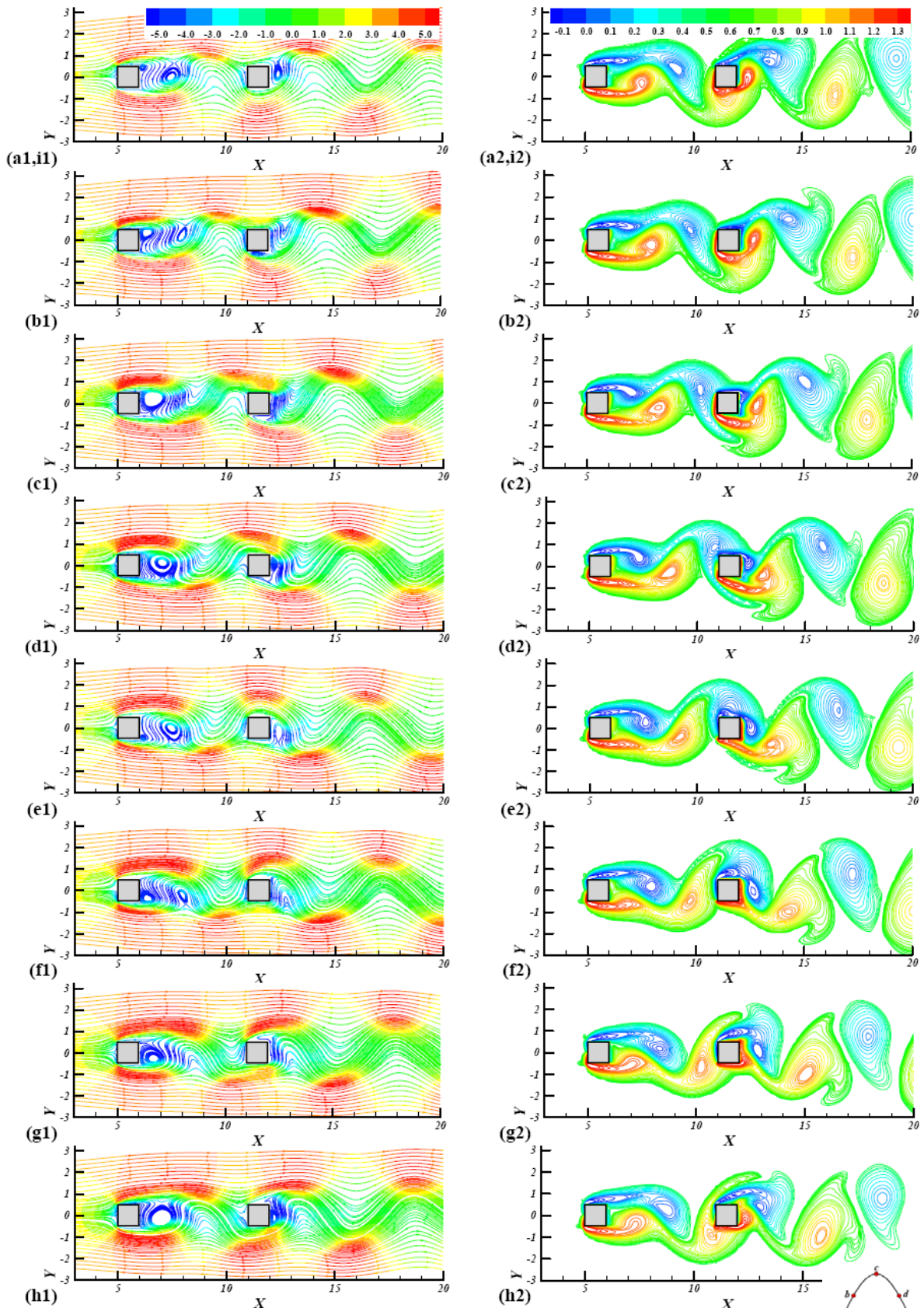
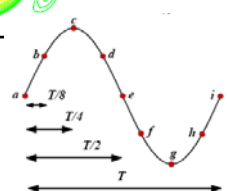


Fig. 4 Instantaneous streamlines colored by x-velocity components (right side graphs) and instantaneous vorticity contours (left side graphs) around the cylinders at nine instants during a period of the vortex shedding (see the opposite graph) for $\text{Re} = 100$



As seen, the x-velocity component level at the center of domain is lowest than other zones. It is caused by the existing of cylinders, boundary layer effects and recirculation flows behind the cylinders. The front sides of cylinders opposite to the incoming flow make the stagnation points that velocity will be zero there and pressure will be so high. The negative value of x-velocity components shows backward flow caused by wake regions.

In general, the critical Reynolds number depends greatly on the distance between the cylinders, inlet flow condition, and the blockage ratio. For example, it is found that the onset Reynolds number for the tandem square cylinders occurs in the range of 35-40, and 40-45 for $B = 5\%$ and $B = 10\%$, respectively. As mentioned before, the results become independent from the blockage effect for $B \leq 5\%$. Thus, it is expected that the accurate critical onset Reynolds number happens at approximately $Re_{cr} = 35 - 40$. In the steady cases, the recirculation length behind the cylinders becomes larger by increasing the Reynolds number and it reaches to the maximum size at the onset Reynolds number. In all the cases,

the recirculation length of the upstream cylinder is larger than the corresponding value for the downstream cylinder.

In the unsteady cases, the upstream recirculation length decreases with increasing Reynolds number, whereas the corresponding value for the downstream cylinder first decreases and then gradually increases. It is reported that the recirculation length for a single square cylinder increases up to approximately the onset of vortex shedding and then decreases and the same trend also occurs for the upstream cylinder in the tandem arrangement. As seen from Figure 5, the level of vorticity is high at the sharp edges of the cylinders.

In addition, the level of vorticity is lesser for downstream cylinder than for the upstream one. The vorticity levels greatly increase with the appearance of the vortex shedding at $Re \geq 40$. By increasing the Reynolds number, the number of separated eddy regions increases. In the other word, the frequency of vortex shedding has been increased by increasing the Reynolds number.

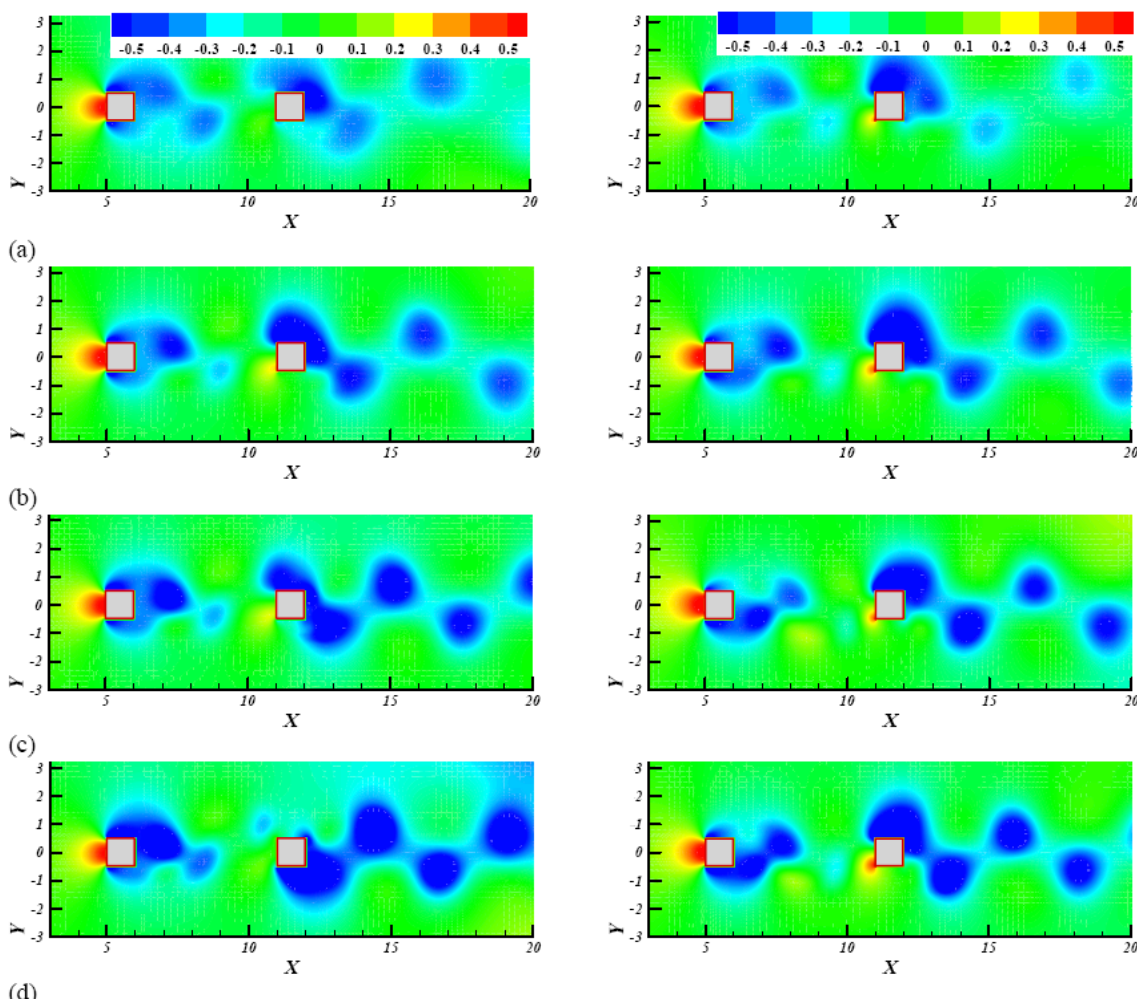


Fig. 5 Instantaneous pressure contours around the cylinders when the maximum lift force acting on upstream cylinder (left side graphs) and on downstream cylinder (right side graphs) for, (a) $Re = 70$ (b) $Re = 100$ (c) $Re = 150$ (d) $Re = 200$

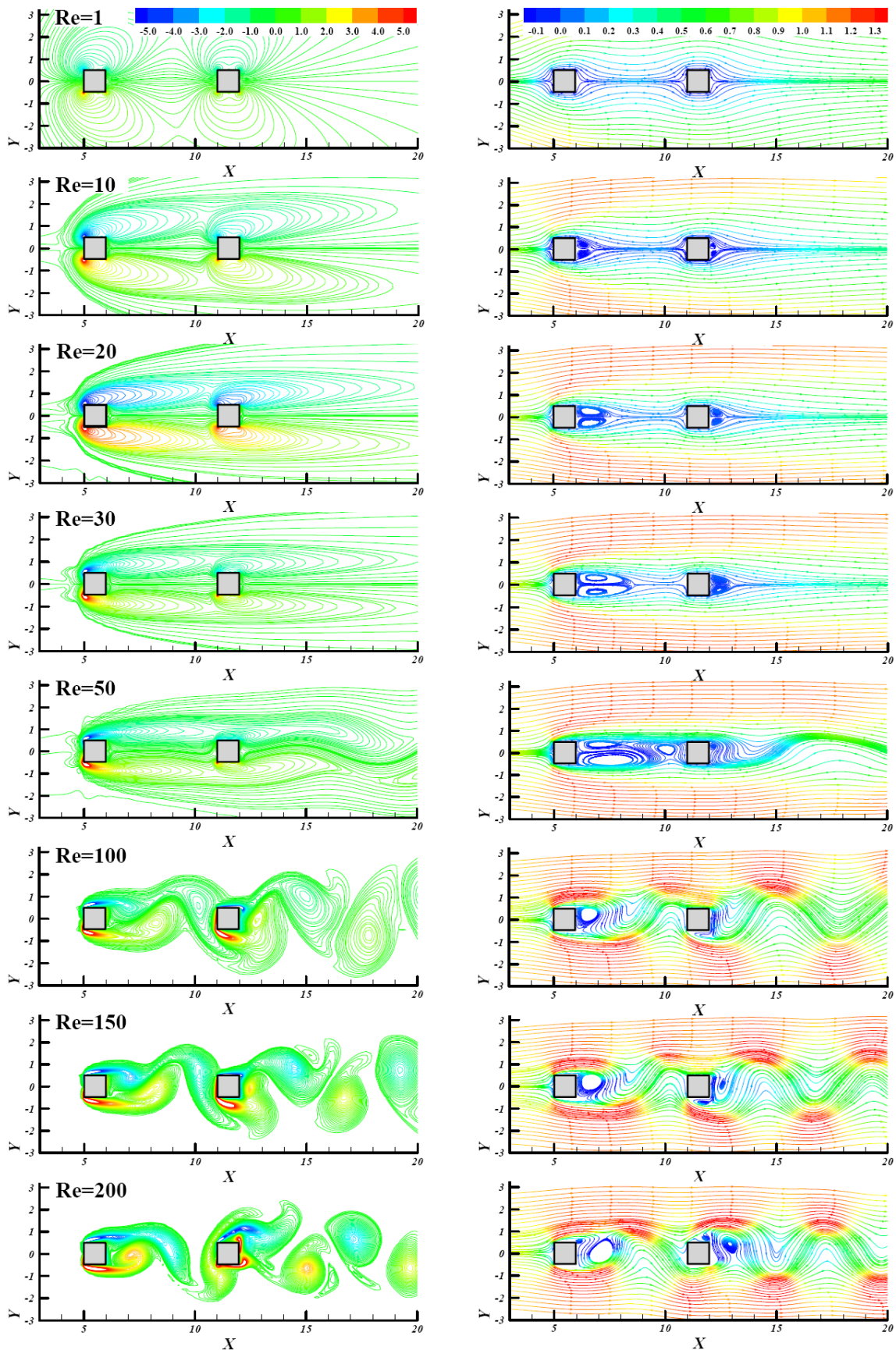


Fig. 6 Instantaneous vorticity contours (left side graphs) and instantaneous streamlines colored by x-velocity components (right side graphs) around the cylinders for different Reynolds numbers

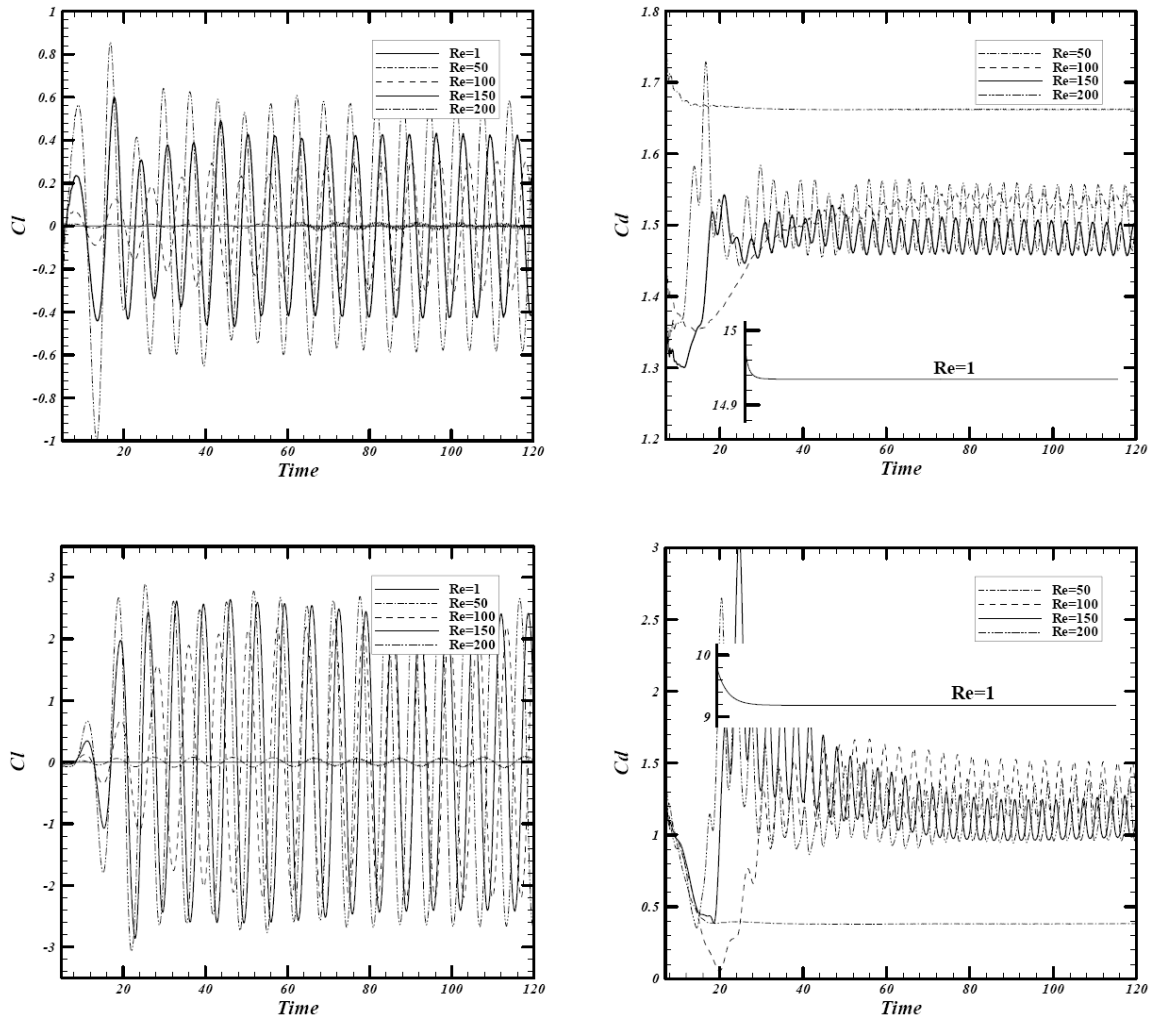


Fig. 7 The time history instantaneous lift and drag coefficients for the upstream cylinder (the upper graphs) and for the downstream cylinder (the lower graphs).

As mentioned earlier, the steady flow becomes an unsteady-periodic flow for $Re \geq 40$, and the alternative forces exert on the cylinders. This is clearly seen in Figure 7, where the time history of the drag and lift forces is shown for upstream and downstream cylinders. It is seen that the flow is steady for $Re \leq 35$ and the aerodynamic forces remain constant during the time, e.g. at $Re = 1, Cd \approx 14.94$ for upstream cylinder and $Re = 1, Cd \approx 9.2$ for downstream cylinder.

In unsteady cases, the forces become periodic and their fluctuations increase with increasing the Reynolds number from the onset one. The mean values of drag coefficient for both cylinders are computed by averaging time history for 10 time period in fully periodic flow. It is seen that the level of the force fluctuations on the downstream cylinder is larger than the corresponding values for the upstream one. This is because the flow interaction of the upstream cylinder with the downstream one causes to amplify the forces and their fluctuations.

As seen in Figure 7, the fluctuations of lift coefficient for both the cylinders are larger than the corresponding values of the drag one.

Figure 8 shows the RMS of aerodynamic forces on right axis for drag and left axis for lift for both the cylinders. As mentioned that, the level of the force fluctuations on the downstream cylinder is larger than the corresponding values for the upstream one.

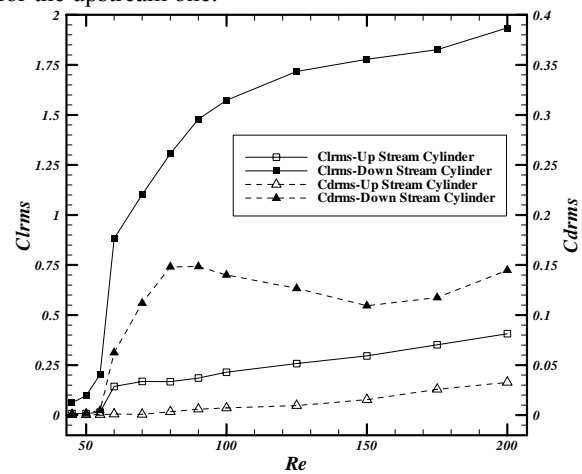


Fig. 8 The RMS of lift and drag coefficients for cylinders versus Reynolds number.

Therefore the values of RMS for downstream cylinder are greater than upstream cylinder. This is because the flow interaction of the upstream cylinder with the downstream one causes to amplify the forces and their fluctuations. As seen in Figure 8, the RMS of lift coefficient for both the cylinders is larger than the corresponding values of the drag one and increased gradually by increasing the Reynolds number.

The vortex shedding of upstream and down stream cylinders is not at the same phase. The spacing between the cylinders and Reynolds number affected highly on form, grow and separation of eddy regions. Figure 9 shows the phase lag of vortex shedding versus the Reynolds number. As seen in this figure, the phase lag increases due to the increasing the Reynolds number.

It is observed that there is a relatively sharp variation in the phase lag of vortex shedding in the range of Reynolds numbers between 55 and 60 due to the change of the flow pattern in the space between the cylinders.

In Figure 10, the drag coefficient and pressure to total drag coefficients ratio versus Reynolds number is shown. At very low Reynolds number ($Re = 1$), there is no flow separation and the drag is predominantly a friction drag.

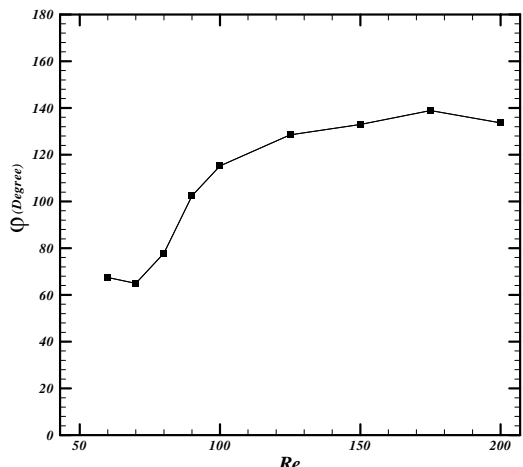


Fig. 9 The phase lag distribution versus the Reynolds number

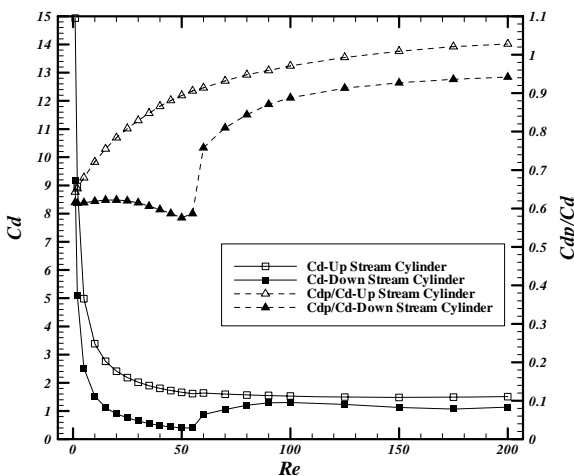


Fig. 10 The variation of drag coefficient (left axis) and the pressure drag to the total drag coefficients ratio (right axis) for the cylinders versus Reynolds number.

As the Reynolds number is increased from $Re=1$, the flow separation occurs and the drag force is a combination of friction and pressure components. By increasing the Reynolds number, the pressure drag starts to increase slowly, whereas the friction drag decreases sharply. Thus, the drag coefficient of both the cylinders drops continuously by increasing the Reynolds number up to $Re=55-60$. The contribution of the pressure drag coefficient is about 80% of the total drag coefficient at $Re=50$. At higher Reynolds number, the drag coefficient of the upstream cylinder is relatively constant, whereas the drag coefficient of the downstream cylinder increases gradually due to the change of flow pattern in the spacing between the cylinders. For $Re>100$, the drag coefficient of the downstream cylinders becomes approximately constant and it approaches the corresponding value of the upstream cylinder. It is important to mention that the location of flow separation points changes from the upstream cylinder trailing edges to their leading edges at $Re>100$.

The recirculation length, defined as the streamwise distance from the base of the cylinder to the re-attachment point along the wake centerline, has an empirical relationship, for the circular cylinder for $4.4 \leq Re \leq 40$ (Zdravkovich [1]), and linear relation for $5 \leq Re \leq 40$ (Sharma [29]) which is shown in Figure 10 for steady flow. Their studies clearly show that the recirculation length for the unconfined square cylinder flow is larger than for its circular counterpart. In the steady cases, the recirculation length behind the cylinders becomes larger by increasing the Reynolds number and it reaches to the maximum size at the onset Reynolds number, see Figures 11 and 6.

In the unsteady cases, the time-averaged recirculation length at the upstream cylinder decreases by increasing the Reynolds number, while the corresponding value for the downstream cylinder first decreases and then gradually increases, see Figure 12. In all the steady and the unsteady cases, the recirculation length of the upstream cylinder is larger than the corresponding value for the downstream cylinder. The size of the recirculation length of both the cylinders draws very close to a same value at approximately $Re = 200$.

Decreasing the recirculation length of the upstream cylinder by increasing the Reynolds number provides more opportunities for the flow to recover pressure before encountering the downstream cylinder. The following expressions for the recirculation length in the steady regime with a maximum deviation of 5% are derived using a linear curve-fit by the least-squares method:

$$\text{Upstream cylinder: } \frac{Lr}{d} = -0.214 + 0.094 \times Re \quad (8)$$

$$\text{Downstream cylinder: } \frac{Lr}{d} = 0.056 + 0.031 \times Re \quad (9)$$

From Figures 11 and 12, it is also seen the recirculation length for a single square or circular cylinder increases up to approximately the onset of vortex shedding and then decreases, and the same trend also occurs for the upstream cylinder in the tandem arrangement.

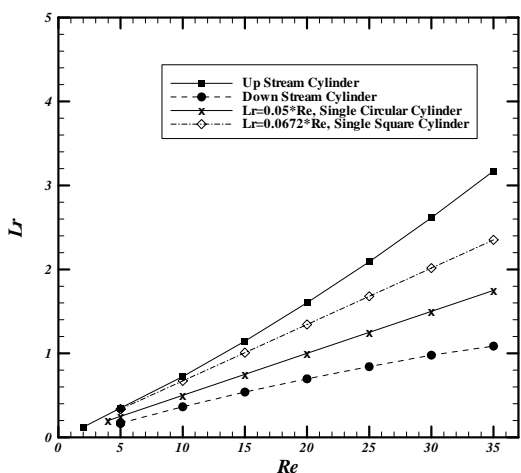


Fig. 11 Variation of recirculation length with Reynolds number for the steady flow regime.

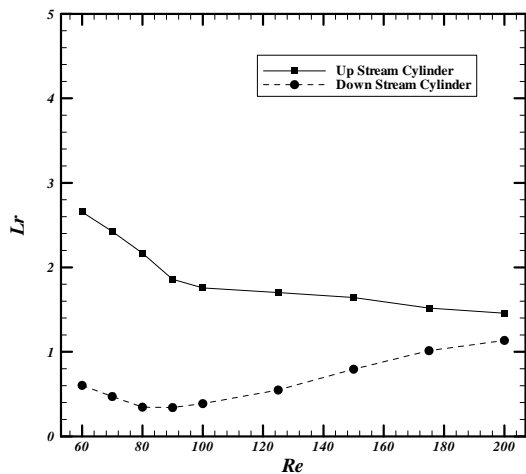


Fig. 12 Variation of recirculation length with Reynolds number for the unsteady periodic flow regime.

IV. CONCLUSION

This study focuses on the unconfined flow characteristics around the tandem square cylinders in the both steady and unsteady-periodic laminar flow regimes ($Re = 1 - 200, G = 5$). The results show that the flow is steady for $Re \leq 35$ and unsteady-periodic for $Re \geq 40$. In terms of separation, three different onset values have been predicted: the first is the onset of separation between $Re = 1$ and $Re = 2$; the second, onset of vortex shedding (with trailing-edge separation) between $Re = 35$ and $Re = 40$; and the third, onset of leading-edge separation between $Re = 100$ and $Re = 125$.

The model of laminar vortex shedding shown by our computed streamlines pattern for the square cylinders matches with that for the single circular and square cylinder as described at literatures. The onset of vortex shedding occurs contemporaneous, but with phase lag. It is found that the level of the force fluctuations on the downstream cylinder is larger than the corresponding values for the upstream one due to the

flow interaction of the upstream cylinder with the downstream one. It is observed that there is a relatively sharp variation in the global parameters of the downstream cylinder in the range of Reynolds numbers between 55 and 60 due to the change of the flow pattern in the space between the cylinders.

With increasing Reynolds number, the recirculation length increases for steady flow, whereas for the mean periodic flow it decreases monotonically. The time-averaged viscous drag coefficient for upstream cylinder is predicted to become negative between $Re = 100$ and $Re = 125$ due to the eddy regions formation close to the top and bottom sides of upstream cylinder. The fluctuating lift and drag forces acting on the downstream cylinder increase when the reattachment position of shear layer precede forward and vice versa.

The fluctuating lift force acting on the upstream cylinder is strictly influenced by the phase of the flow pattern of the downstream cylinder. When the phase of the flow pattern of the downstream cylinder coincides with the phase of the flow pattern of the upstream cylinder, the fluctuating lift force acting on the upstream cylinder become maximum, and when the phase of the flow pattern of the downstream cylinder is out-of-phase with the downstream cylinder's flow pattern, the fluctuating lift force becomes minimum.

NOMENCLATURE

B	blockage ratio
Cd	total drag coefficient
Cdf	viscous drag coefficient
Cdp	pressure drag coefficient
Cdrms	root mean square (RMS) of the drag coefficient
Cl	total lift coefficient
Clf	lift coefficient viscous
Clp	pressure lift coefficient
Clrms	root mean square (RMS) of the lift coefficient
d	width of square cylinders
F _d	total drag force
F _{df}	viscous drag force
F _{dp}	pressure drag force
F _I	total lift force
F _{lf}	viscous lift force
F _{lp}	pressure lift force
G	spacing between the cylinders
H	width of computational domain
L	length of computational domain
L _r	recirculation length
p	pressure
P	non-dimensional pressure
Re	Reynolds number
t	time
u	streamwise velocity
U	non-dimensional streamwise velocity
v	cross-stream velocity
V	non-dimensional cross-stream velocity
x	streamwise dimension coordinate
X	non-dimensional streamwise dimension coordinate

X_d	non-dimensional streamwise distance between the rear side of the downstream cylinder and the exit plane
X_u	non-dimensional streamwise distance between the inlet plane and the front side of the upstream cylinder
y	cross-stream dimension of coordinate
Y	non-dimensional cross-stream dimension of coordinates
Greek letters	
ρ	fluid density
τ	non-dimensional time
ν	fluid kinematic viscosity
ϕ	phase lag
ω_z	vorticity in the z-direction

ACKNOWLEDGMENT

This work was supported by the Islamic Azad University, Neyriz Branch.

REFERENCES

- [1] M.M. Zdravkovich, "Flow around circular cylinders," Oxford University Press, New York, 1997.
- [2] M.M. Zdravkovich, "Flow-induced oscillations of two interfering circular cylinders," Journal of Sound and Vibration, 101, 1985, pp.511–521.
- [3] M. Mani and S. Mahjoob, "A comparative investigation into aerodynamic performances of two set finned bodies with circular and non circular cross sections," WSEAS/IASME International Conference on Fluid Mechanics, Miami, Florida, USA, January 18-20, 2006, pp. 1-6
- [4] D. Portugaels, J. Anthoine and D. Olivari , "Determination of aerodynamic force coefficients of octagonal lighting columns from wind tunnel experiments," 5th IASME / WSEAS International Conference on Fluid Mechanics and Aerodynamics, Athens, Greece, August 25-27, 2007, pp. 81-89
- [5] S.R Sabbagh, F. Meysami and N.E. Mastorakis , "Simulation of Wind Pressure on Circular Cylinder at Super-Critical Reynolds Number," 11th WSEAS International Conference on APPLIED MATHEMATICS, Dallas, Texas, USA, March 22-24, 2007, pp. 256-260
- [6] F.K. Benra and H.J. Dohmen, "Application of simulation methods considering the interaction between fluid and structure," 7th IASME/WSEAS International Conference on FLUID MECHANICS and AERODYNAMICS, Moscow, Russia, 2009, pp. 116-121
- [7] C.H.K. Williamson, "Three-dimensional wake transition. Journal of Fluid Mechanics," 328, 1996, pp.345–407.
- [8] M. Matsumoto, "Vortex shedding of bluff bodies: A Review," Journal of Fluids and Structures, 13, 1999, pp. 791-811.
- [9] Günter Schewe, "Reynolds-number effects in flow around more-or-less bluff bodies," Journal of Wind Engineering and Industrial Aerodynamics, 89, 2001, pp.1267-1289.
- [10] M. Sariglu and T. Yavuz, "Subcritical flow around bluff bodies," AIAA, 40, 7, 2002, pp. 1257-1268.
- [11] A. Sohankar, "Flow over a bluff body from moderate to high Reynolds numbers using large eddy simulation," Computers and Fluids, 35, 2006, pp. 1154–1168.
- [12] K. Tatsutani, R. Devarakonda and J.A.C Humphrey, "Unsteady flow and heat transfer for cylinder pairs in a channel," International Journal of Heat and Mass Transfer, 13, 1993, 3311-3328.
- [13] A. Valencia, "Unsteady flow and heat transfer in a channel with a built-in tandem of rectangular cylinders," Numerical Heat Transfer, Part A, 26, 1996, pp. 613-623.
- [14] A. Valencia, "Numerical study of self-sustained oscillatory flows and heat transfer in channels with a tandem of transverse vortex generators," Heat and Mass Transfer, 33, 1998, pp. 465-470.
- [15] R. Devarakonda and J.A.C. Humphrey, "Interactive computational and experimental methodologies in cooling of electronic components," Computer Mechanics Laboratory, Technical Report No. 92-008, University of California, Berkeley, CA, 1992.
- [16] R. Devarakonda, "Experimental and numerical investigation of unsteady bluff body flows," Ph.D. Dissertation, University of California at Berkeley, Berkeley, CA, 1994.
- [17] J.L. Rosales, A. Ortega and J.A.C. Humphrey, "A numerical simulation of the convective heat transfer in confined channel flow past square cylinders: comparison of inline and offset tandem pairs," International Journal of Heat and Mass Transfer, 44, 2001, pp. 587-603.
- [18] L.W. Zhang, S. Balachandar, D.K Tafti and F.M. Najjar, "Heat transfer enhancement mechanisms in inline and staggered parallel-plate fin heat exchangers," International Journal of Heat and Mass Transfer, 40, 1997, pp. 2307.
- [19] N.C. Dejong, L.W. Zhang, A.M. Jacobi, S. Balachandar and D.K. Tafti, "A complementary experimental and numerical study of flow and heat transfer in offset strip-fin heat exchangers," Journal of Heat Transfer, 120, 1998, pp.690.
- [20] C.H. Liu and J.M. Chen, "Observations of hysteresis in flow around two square cylinders in a tandem arrangement," Journal of Wind Engineering and Industrial Aerodynamics, 90, 2002, pp.1019–1050.
- [21] Md.M. Alam, M. Moriya, K. Takai, H. Sakamoto,, "Suppression of fluid forces acting on two square prisms in a tandem arrangement by passive control flow," Journal of Fluids and Structures, 16, 2002, pp.1073–1086.
- [22] S.C. Yen, K.C. San, T.H. Chuang, "Interactions of tandem square cylinders at low Reynolds numbers," Experimental Thermal and Fluid Science, 32, 2008, pp.:927–938.
- [23] J. Mizushima and T. Akinaga, "Vortex shedding from a row of square bars," Fluid Dynamics Research, 32, 2003, pp. 179-191.
- [24] A. Sohankar, C. Norberg and L. Davidson, "Low-Reynolds-number flow around a square cylinder at incidence: study of blockage, onset of vortex shedding and outlet boundary condition," International Journal for Numerical Methods in Fluids, 26, 1998, pp.39-56.
- [25] A. Etmianan, "Numerical simulation of fluid flow and heat transfer over two square cylinders," M.Sc. Thesis, Mechanical Engineering Department, Yazd University, Yazd, Iran, 2007.
- [26] J.F. Thompson, Z.U.A. Warsi and C.W. Mastin, "Numerical grid generation, foundations and applications," Elsevier Science, New York, 1985, pp.305-310.
- [27] K.M. Kelkar and E.F. Patankar, "Numerical prediction of vortex shedding behind a square cylinder," International Journal for Numerical Methods In Fluids, 14, 1992, pp.327.
- [28] A. Sohankar, C. Norberg and L. Davidson, Dec. "Numerical simulation of unsteady flow around a square two-dimensional cylinder," In. Proc. 12th Australasian Fluid Mechanics Conference, The University of Sydney, Australia, pp. 517-520,1995.
- [29] A. Sharma and V. Eswaran, "Heat and fluid flow across a square cylinder in the two-dimensional laminar flow regime," Numerical Heat Transfer, Part A, 45, 2004, pp.247-269.

Amin Etmianan was born in 1 September 1982 at Shiraz. He graduated from Persian Gulf University on Fluid Mechanics in 2004. Then he passed the M.Sc. course at Yazd University on Fluid Mechanics/Energy Conversion in 2007. Most of the time, he was very active at class and got top marks in some courses. He participated in some regional, national and international conferences on Mechanical Engineering and related fields. But his major field of study is turbulent fluid flow and heat transfer. He passed practical course at Boushehr Gas Power Plant.

He has held positions on the Mechanical Engineering Department of the Islamic Azad University and he was the head of Mechanical Engineering Department for two years at Neyriz Branch. He knows some sports such as; Swimming, Ping-Pong and Chess. In addition to some research papers, he authored; "Determination of aerodynamic forces acting on equal square cylinders." the 11th Fluid Dynamics Conference in 2008, "Convection heat transfer from a square cylinder at incidence in the laminar flow regime," Journal of Mechanical Engineering, in 2009, "Determination of fluctuating forces acted on cylinders and heat transfer from them in the turbulent flow regime," Journal of Mechanical Engineering in 2010.

Now, he is a licensee member of Iranian Engineering Organization in Construction Activities. Also, he was the chairman of the Regional Conference on Mechanical Engineering in 2009 and received the Top Authors Award. He earned the Top Authors Award in 2008 in National Conference on Mechanical Engineering too.